Ind. J. Pharm. Edu. Res., 2024; 58(3):802-813.
https://www.ijper.org

Original Article

Inhibiting Cancer Progression through Targeting HDAC2 with Novel Ligands: A Dynamic Insights through Virtual Screening and Simulation

Ayyub Ali Patel[1], Hani Alothaid[2], Ayaz Khurram Mallick[1], Adel Ibrahim Alalawy[3], Rasha Tarek Mirdad[4], Mahmoud Tarek Mirdad[5], Mohammed Tarek Mirdad[5], Marya Ahsan[6], Mohammed Tarique[7,*]

[1]Department of Clinical Biochemistry, College of Medicine, King Khalid University, Abha, SAUDI ARABIA.
[2]Department of Basic Medical Science, Faculty of Applied Medical Sciences, Al-Baha University, SAUDI ARABIA.
[3]Department of Biochemistry, Faculty of Science, University of Tabuk, Tabuk 71491, SAUDI ARABIA.
[4]Department of Surgery, King Khalid University, Abha, KINGDOM OF SAUDI ARABIA.
[5]Department of Clinical Biochemistry, College of Medicine, King Khalid University, Abha, SAUDI ARABIA.
[6]Department of Pharmacology, College of Medicine,Imam Mohammad Ibn Saud Islamic University (IMSIU), Riyadh, SAUDI ARABIA.
[7]Almanac Life Science India Private Limited, New Delhi, INDIA.

ABSTRACT

Background: Cancer is a multifaceted disease characterized by uncontrolled cell growth and represents a significant global health challenge. The intricate origins of cancer involve various factors that may act independently or collectively, contributing to its initiation and progression and resulting in the dynamic nature of the disease. **Aim:** The current focus of research is to elucidate the role of histone acetylation in cancer progression. **Materials and Methods:** A key area of interest is histone deacetylation, which intensifies ion-based interactions between negatively charged DNA and positively charged histones. Histone deacetylation, specifically the removal of acetyl groups from histone proteins by Histone Deacetylase 2 (HDAC2), plays a pivotal role in regulating gene expression. The primary objective of this study was to identify molecular inhibitors targeting HDAC2 through Structure-Based Virtual Screening (SBVS) using an extensive MCULE chemical compound database. After the application of stringent filters, 100 promising compounds were selected for further investigation. **Results:** Docking simulations using DockThor revealed 16 molecules with superior free binding energies compared to the control (entinostat). Subsequently, ten compounds meeting the Absorption, Distribution, Metabolism and Excretion (ADME) rules were chosen based on the Egan-Egg permeation predictive model. The top two ligands, along with the positive control entinostat, underwent a five-nanosecond molecular dynamics simulation. The evaluation criteria included toxicity profiling, physiochemical properties, lipophilicity, solubility, pharmacokinetics, druglikeness, medicinal chemistry attributes, Root Mean Square Deviation (RMSD), Root Mean Square Fluctuation (RMSF) and Radius of Gyration (Rg). **Conclusion:** Through these analyses, ligand MCULE-5097730104-0-3 emerged as a promising HDAC2 inhibitor, exhibiting potential efficacy in combating cancer progression.

Keywords: HDAC2, Cancer, RMSD, SBVS, MD Simulation.

Correspondence:
Dr. Mohammed Tarique
Almanac Life Science India Private Limited, New Delhi, INDIA.
Email: tariqueaiims@gmail.com

Received: 28-12-2023;
Revised: 21-02-2024;
Accepted: 02-05-2024.

INTRODUCTION

Cancer, a complex group of diseases characterized by uncontrolled cell growth, poses a significant global health challenge. Its widespread impact is evidenced by the high incidence and mortality rates reported worldwide.[1] Indeed, recent epidemiological data indicate that millions of new cases are diagnosed annually, with mortality rates further emphasizing the seriousness of this condition.[2] According to a 2019 report by the World Health Organization (WHO), cancer is the leading cause of death in 112 of 183 countries for individuals under the age of 70[2]. This grim statistic highlights the profound effect of cancer on premature mortality, which is closely tied to socioeconomic factors at the national level.[3] Cancer development results from complex interactions within the cellular environment involving a range of factors.[4,5] These include genetic mutations involving oncogenes and tumor suppressor genes, dysregulation of signaling pathways leading to uncontrolled cell proliferation, apoptotic resistance, angiogenesis initiation, metastasis, genomic instability due to defective DNA repair mechanisms, hormonal influences such as estrogen imbalance in breast cancer, chronic

DOI: 10.5530/ijper.58.3.88

inflammation and epigenetic alterations.[6] These elements, whether acting individually or in combination, contribute to the initiation and progression of cancer, thereby shaping its complex landscape. Environmental exposure and lifestyle choices also play a crucial role in this intricate interplay. The ever-evolving field of cancer research continues to provide new insights, offering hope for improved patient outcomes in the future.[7,8]

One of the most extensively researched epigenetic modifications involves DNA methylation or hypermethylation of tumor suppressor genes. Knowledge of histone modifications has greatly enhanced efforts to combat cancer development. Histone acetylation, a component of histone modifications, also plays a key role in chromatin remodeling and gene transcription regulation.[9] Acetylation occurs because of an imbalance between Histone Acetyltransferase (HAT) and Histone Deacetylase (HDAC). Histone Deacetylase 2 (HDAC2) is a crucial member of the histone deacetylase enzyme family and is responsible for regulating gene expression by removing acetyl groups from histone proteins. Histone deacetylation enhances ion-based interactions between negatively charged DNA and positively charged histones.[9] HDACs also form corepressor complexes with nuclear receptors in the absence of ligands and are involved not only in the deacetylation process but also in the regulation of non-histone proteins, which can influence cellular homeostasis through apoptosis, differentiation and cell cycle progression.[10,11] Entinostat, also known as SNDX-275, is an investigational Histone Deacetylase inhibitor (HDACi) with potential applications in cancer therapeutics. HDAC inhibitors, including entinostat, modulate the activity of histone deacetylase enzymes, which are crucial for the regulation of gene expression. Despite promising results in preliminary studies and early-phase clinical trials, the evaluation of entinostat efficacy and safety across various cancer types in larger clinical trials has affected its current position in cancer treatment. The limited adoption or absence of entinostat in cancer drug development is attributed to several factors, such as its reduced efficacy compared to combination therapies, safety and tolerability concerns, considerations regarding cellular specificity targeting cancer cells and challenges associated with obtaining regulatory approval.

Our ongoing research efforts are centered on the identification of a lead compound that exhibits potential anti-cancer properties. As a pioneering innovation, our research aims to unveil the mechanisms by which this compound may interfere with cancer pathways, thereby offering a promising avenue for therapeutic interventions. As we embark on this endeavor, our ultimate objective is to make a significant contribution to the field and, subsequently, to the lives of cancer patients.[9-11]

MATERIALS AND METHODS

Obtaining and Optimizing the Structure of HDAC2 Protein

The crystal structure of HDAC2 (6WBW) in three dimensions was obtained at a resolution of 1.70 Å from the RCSB Protein Data Bank (PDB).[12,13] To generate a suitable three-dimensional input file for docking tools, the protein portion of the crystal structure was selected and unwanted heteroatoms, ions and molecular entities were eliminated. Subsequently, the structural arrangement was enhanced and refined using the CHARMm force field.[14]

High-Throughput Structure-Based Virtual Screening (SBVS)

The pursuit of essential small molecules was facilitated through the Mcule online drug discovery platform, which employs a high-throughput Structure-Based Virtual Screening (SBVS) process. This SBVS process entailed the establishment of fundamental property filters that were specifically aligned with the Lipinski Rule of Five (ROF: molecular weight≤500 Da; hydrogen bond donor count≤5; hydrogen bond acceptor count≤10; LogP≤5). In addition to these criteria, further considerations were considered, including a chiral center count≤3, rotatable bond count≤4, N and O atom count≤10, heavy atom count≥10 and a limitation on the number of rings (≤3). The SBVS search parameters were configured with a sample size of 100,000, diversity selection of 1000 and similarity threshold of 0.85. Exploration was performed using the Open Babel linear fingerprint search algorithm.[15,16]

Acquisition and Refinement of HDAC2 Inhibitor Structure

The histone deacetylase 1 (HDAC2) inhibitor entinostat ($C_{21}H_{20}N_4O_3$; CID: 4261) was obtained from the PubChem database in a standard format. To improve the analytical capabilities, the SDF-2D file representation of the inhibitor was converted to a PDB-3D file format using BIOVIA Discovery Studio. The optimization protocol applied to the inhibitor followed the procedures discussed for receptor molecules.[17,18]

Molecular Interactions through Computational Docking with DockThor

Molecular interactions between HDAC2 and the compounds were investigated using DockThor,[19] with the apo protein segment of HDAC2 designated as the reference target. A grid size of 40 Å was used for the x-, y- and z-axes. The protein-ligand binding site was defined by a grid box with variable grid points along the x (61.1155 Å), y (26.6795 Å) and z (-2.2715 Å) axes. The minimum free energy of binding (ΔG) was chosen as the criterion for identifying the optimal binding affinity and position for each ligand molecule docked within the active site of HDAC2.[20]

Segregation of Toxicophores

After molecular docking, the top 100 molecules were subjected to toxicity profiling using the Mcule Toxicity Checker. This involves employing SMARTS (SMILES Arbitrary Target Specification) toxic matching rules to evaluate the existence of potentially harmful substructures, scaffolds, or moieties, known as toxicophores, within chemical compounds.[21,22]

Depiction of Absorption, Distribution, Metabolism and Excretion (ADME) Properties

The evaluation of compounds as potential drugs and their impact on the human body requires a thorough assessment of their absorptive, distributive, metabolic and excretory properties. This process involves categorizing compounds based on their pharmacokinetic attributes and adherence to ADME criteria, which are critical for successful outcomes in laboratory experiments.[23] To assess the ADME characteristics of the compounds, the SwissADME web tool was used, which considers factors such as drug-likeness, medicinal chemistry attributes, lipophilicity and physicochemical properties.[24,25]

Stability Assessment via Molecular Dynamics (MD) Simulations

To evaluate the stability of the protein-ligand complexes, the GROMACS grep module was employed to extract ligands from their respective complexes and the CHARMm General Force Field (CGenFF) server was utilized for topology and forcefield parameter assignment. The GROMACS 5.1.2 software facilitated computational simulations to assess the stability of the two most promising protein-ligand docked complexes and the positive control.[14,26] The topology of HDAC2 was generated using the pdb2gmx segments in the GROMACS package and structural coordinates for the top three hits were obtained using the CGenFF tool.[27] Each molecular complex was enclosed within a dodecahedron box filled with water molecules, establishing a 10 Å protective margin around the complex. The complex charges were neutralized and sodium and chloride ions were introduced to maintain a biological concentration of 0.15 M. The steepest descent algorithm was then employed for an extensive 250,000-step energy-minimization procedure. The temperature of the system was gradually increased from 0 to 300 K over a ten ns equilibration period, adhering to Standard Temperature and Pressure (STP) conditions. Once equilibrium was achieved, particle mesh was applied using the Ewald scheme. Various GROMACS modules have been utilized to scrutinize the stability of the identified molecules by employing metrics such as Root-Mean-Square Deviation (RMSD), Root-Mean-Square Fluctuation (RMSF) and Radius of gyration (Rg).[28]

RESULTS

Structure-Based Virtual Screening (SBVS) was conducted after implementing a comprehensive screening protocol using the Mcule online drug discovery platform. The process commenced with the acquisition of a vast dataset of 2,208,042 ligand molecules.

Table 1: Binding Energies and Molecular Interactions of Ligand Hits Passing Toxicity Checker and the Reference Inhibitor Entinostat.

Sl. No.	Ligand	Binding energy (kcal/mol)	Types of molecular interactions
1.	MCULE-1047982559-0-12	-9.2	Van der Waals (Vdw), Hydrogen bonds, Carbon Hydrogen bond, carbon Hydrogen bonds, Halogen (Fluorine), Pi-Pi T shaped, Pi-Alkyl.
2.	MCULE-1153881170-0-3	-8.7	Vdw, Hydrogen bonds, Carbon Hydrogen bond, halogen (Fluorine), Amide-Pi stacked, Pi-Alkyl, Alkyl.
3.	MCULE-1537658116-0-1	-8.8	Vdw, Hydrogen bonds, Carbon Hydrogen bonds, Halogen (Fluorine), Pi-Alkyl, Alkyl.
4.	MCULE-2009158975-0-4	-8.5	Vdw, Hydrogen bonds, Carbon Hydrogen bond, Pi-Alkyl, Alkyl.
5.	MCULE-3797459988-0-5	-8.8	Vdw, Hydrogen Bond, pi-Cation, Pi-Sigma, Pi-Pi stacked, Pi-Alkyl.
6.	MCULE-4334038893-0-3	-8.6	Vdw, Hydrogen bonds, Halogen (Fluorine), Pi-Anion, Pi-Pi T shaped, Pi-Alkyl.
7.	MCULE-6503598615-0-2	-8.9	Vdw, Hydrogen bonds, Pi-Anion, Pi-Pi sigma, Pi-Pi Stacked, Pi-Alkyl.
8.	MCULE-6610635460-0-144	-8.6	Vdw, Hydrogen bonds, Carbon Hydrogen bonds, Alkyl, Pi-Alkyl.
9.	MCULE-6885931637-0-1	-9.0	Vdw, Hydrogen bonds, Alkyl, Pi-Alkyl.
10.	MCULE-5097730104-0-3	-9.7	Vdw, Hydrogen Bonds, Carbon Hydrogen bonds, Pi-Sigma, Pi-Pi Stacked, Pi-Pi T-shaped, Pi-Alkyl.
11.	Entinostat (Control)	-8.5	Vdw, Hydrogen bonds, carbon Hydrogen bonds, Pi-Cation, Pi-Pi stacked, Pi-Pi T shaped, Pi-Alkyl.

Subsequently, a refined subset dataset of top-performing ligands was identified through stringent criteria, including adherence to Lipinski's Rule of Five (RO5), drug-likeness parameters and considerations of N and O atoms, as detailed in the methodology section.[29,30]

Following the initial screening, the top 100 ligands were further refined through toxicity profiling and assessment of the binding free energy. This meticulous selection process resulted in the identification of two investigational ligands with ΔG values better than the control molecule entinostat (-8.5 kcal/mol). These lead ligands, characterized by ΔG values of -9.7 kcal/mol and -9.2 kcal/mol, respectively, were prioritized for subsequent simulation studies.

Toxicity Assessment for SBVS-Identified Candidates

Assessing the pharmacokinetic properties of a drug is crucial in biological processes and can greatly affect subsequent stages, necessitating additional resources. In the early stages of drug development, it is essential to eliminate compounds that may possess carcinogenic, mutagenic, or toxic scaffolds or toxicophores.[24,31] Through this screening process, ten of the initial 100 ligands (Table 1) were identified, demonstrating the absence of toxic moieties or problematic scaffolds.

Molecular Docking Analysis Using DockThor

In this study, the investigators utilized the DockThor tool to assess the binding affinities of various ligands, including the reference inhibitor entinostat, within the HDAC2 binding pocket. The calculated binding free energy (ΔG) values, which ranged from -9.7 kcal/mol to -8.5 kcal/mol, are listed in Table 1. DockThor, developed by the Molecular Modeling of Biological Systems Group Brazil, is a noncovalent molecular docking tool that employs topology files for ligands and cofactors along with a specific protein input file containing atom types and partial charges from the MMFF94S49 force field. The ligand input was generated using the Open Babel Chemical Toolbox, which involves the processing of partial charges and atom types using the MMFF94S force field. This includes identifying Rotatable Bonds (RBs) and terminal hydroxyl groups, as well as computing properties essential for assessing intramolecular interactions.[32] Maintaining consistency with the ADV, the grid box center and size along the x-, y- and z-axes were specified. Default values were set for the grid spacing and genetic algorithm parameters, including the number of evaluations, population size, number of runs and seed. The resulting binding affinity and ranking of ligands were expressed using the DockThor score, analogous to ΔG. A comparative analysis was conducted by contrasting the docked complexes of the predicted ligands with HDAC2 to the reference drug entinostat.[33-35] The ΔG value for the interaction between entinostat and the HDAC2 binding pocket was determined to be -8.5 kcal/mol. This interaction involved 14 residues and various binding interactions, including van der Waals forces, conventional hydrogen bonds, carbon-hydrogen bonds, Pi-Cation bonds, Pi-Pi T-shaped interactions, Pi-Pi Stacked interactions and Pi-Alkyl interactions, as illustrated in Figure 1. Notably, only ten ligand hits from the toxicity checker

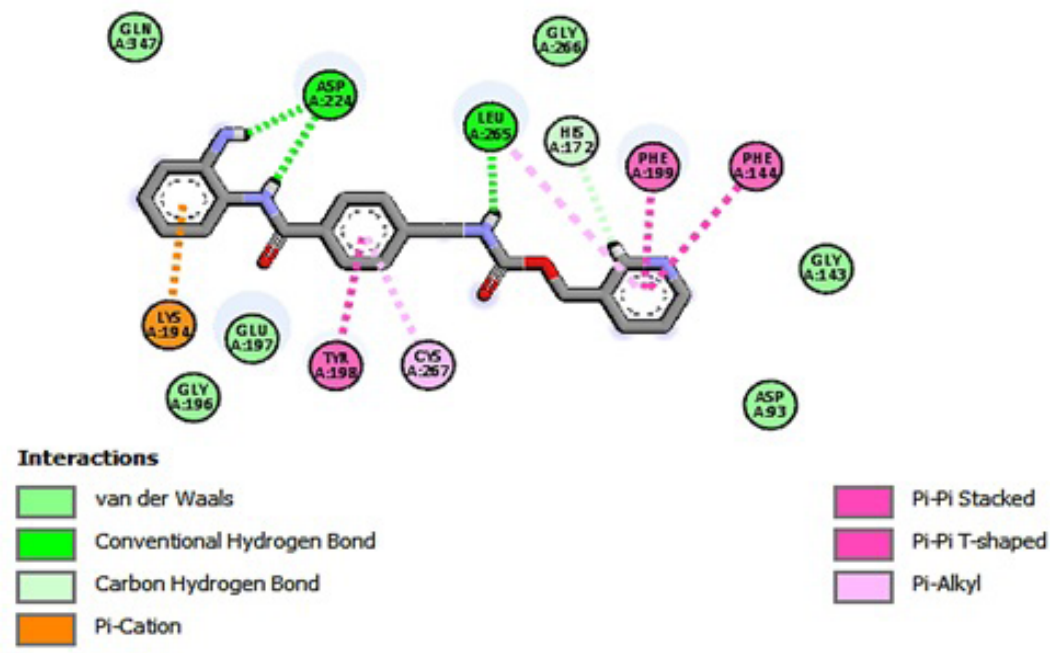

Figure 1: 2D Illustration depicting the engagement between HDAC2 and the control molecule (Entinostat) during protein-ligand docking. Various molecular forces, including Van der Waals (Vdw), Hydrogen Bonds (HBs), Carbon-Hydrogen Bonds (CHB), Pi-Cation, Pi-Pi T-shaped, Pi-Pi Stacked and Pi-Alkyl, are highlighted to showcase the intricate interactions between the protein and ligand.

exhibited ΔG values equal to or lower than that of entinostat, as shown in Table 1.

The results of the hydrogen bond analysis revealed that only two compounds, namely MCULE-5097730104-0-3 and MCULE-1047982559-0-12, showed three and one hydrogen bond, respectively, in comparison to the reference molecule, entinostat, which displayed three hydrogen bonds. Subsequently, the selection of compounds was based on maximizing the presence of hydrogen bonds and robust binding affinity relative to control molecules. Notably, MCULE-5097730104-0-3, with a ΔG value of -9.7 kcal/mol, interacted with 11 residues through seven distinct binding interactions, including van der Waals forces, hydrogen bonds, carbon-hydrogen bonds, Pi-Sigma interactions, Pi-Pi Stacked interactions, Pi-Pi T-shaped interactions and Pi-alkyl interactions (Figure 2). Similarly, MCULE-1047982559-0-12, with a ΔG value of -9.2 kcal/mol, engaged with 14 residues through six different binding interactions, namely Van der Waals forces, hydrogen bonds, carbon-hydrogen bonds, Halogen (Fluorine) based bonds, Pi-Pi T-shaped interactions and Pi-Alkyl interactions (Figure 3).

Comparatively, these ligands demonstrated favorable hydrogen bond interactions and lower ΔG values, indicating potentially stronger binding affinities with HDAC2 residues than the reference molecule entinostat. These findings suggest promising candidates for further consideration in drug development.

HIA and BBB Permeation with Egan-Egg Filtration

The Egan-Egg model, a crucial component of Absorption, Distribution, Metabolism and Excretion (ADME) descriptors, has been utilized to predict the suitability of ligands in terms of passive Human Intestinal Absorption (HIA) and permeation through the Blood-Brain Barrier (BBB). This model distinguishes between distinct regions, represented by yellow and white, which correspond to physicochemical spaces associated with noteworthy BBB permeation and Gastrointestinal (GI) absorption, respectively.[36,37]

Among the ligand hits assessed, namely MCULE-1047982559-0-12, MCULE-1153881170-0-3, MCULE-1537658116-0-1, MCULE-2009158975-0-4, MCULE-3797459988-0-5, MCULE-4334038893-0-3, MCULE-6503598615-0-2, MCULE-6610635460-0-144, MCULE-6885931637-0-1, MCULE-5097730104-0-3, all exhibited plausible HIA permeation. However, it is worth noting that none of the ligand hits demonstrated BBB permeability. The significance of human intestinal absorption and blood-brain barrier permeation in Computer-Aided Drug Design (CADD) cannot be overstated. HIA permeation is a critical parameter as it reflects the potential for a drug to be absorbed in the human gastrointestinal tract, influencing its bioavailability and overall efficacy. Conversely, BBB permeation is a critical consideration, especially for drugs that target the central nervous system. The inability of the ligand to exhibit BBB permeation suggests potential limitations

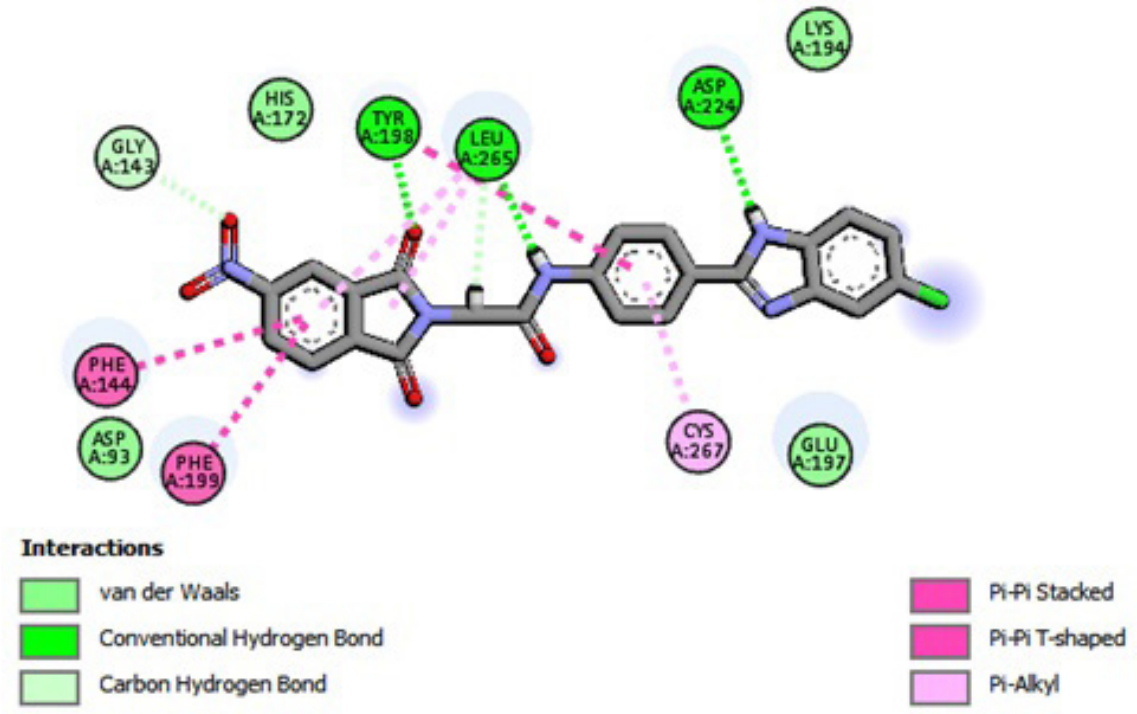

Figure 2: 2D Illustration presenting a 2D depiction of the molecular interactions between HDAC2 and MCULE-5097730104-0-3 in the course of protein-ligand docking. The figure highlights various molecular forces, including Van der Waals (Vdw), Hydrogen Bonds (HBs), Carbon-Hydrogen Bonds (CHB), Pi-Sigma, Pi-Pi Stacked, Pi-Pi T-shaped and Pi-Alkyl, emphasizing the detailed and intricate engagement between the protein and the ligand.

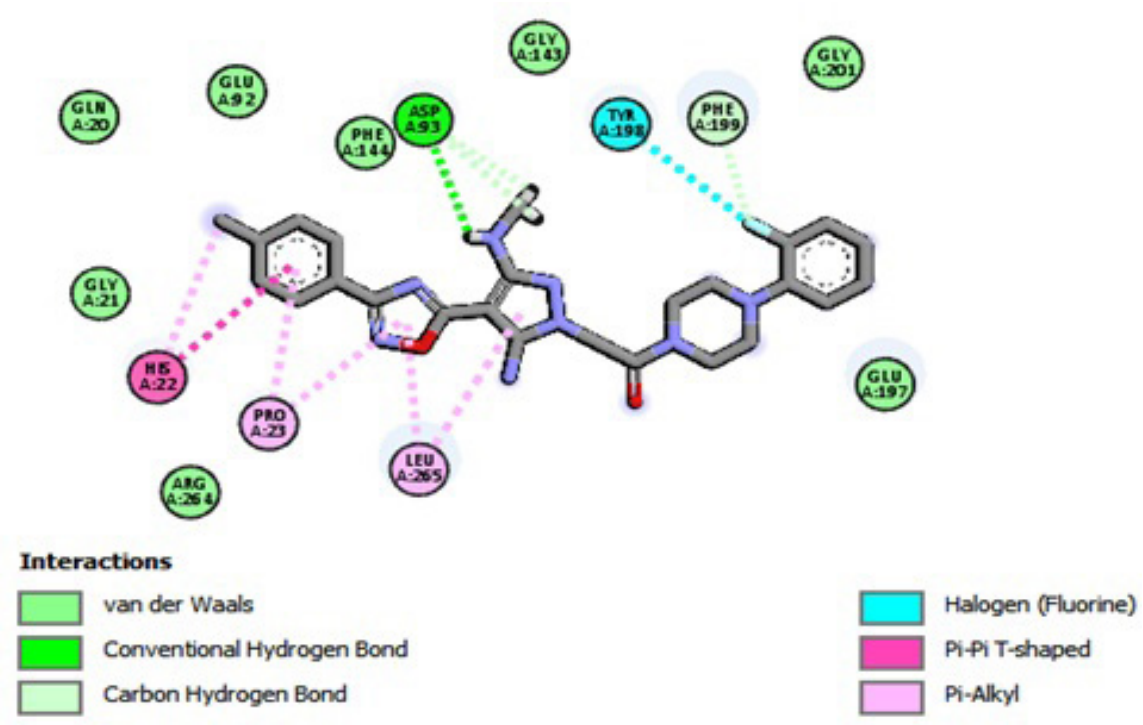

Figure 3: 2D Illustration presenting a 2D depiction of the molecular interactions between HDAC2 and MCULE-1047982559-0-12 in the course of protein-ligand docking. The figure highlights various molecular forces, including Van der Waals (Vdw), Hydrogen Bonds (HBs), Carbon-Hydrogen Bonds (CHB), Halogen (fluorine), Pi-Pi T-shaped and Pi-Alkyl, emphasizing the detailed and intricate engagement between the protein and the ligand.

in its ability to access the brain, influencing its utility in drug development. This information is crucial for rational drug design and aids in prioritizing compounds with optimal pharmacokinetic properties for further development.

Analysis of Physicochemical Characteristics

Molecular properties such as Molecular Weight (MW), FCsp3 hybridization, Rotatable Bonds (RB), Hydrogen Bond Acceptor (HBA), Hydrogen Bond Donor (HBD) and Total Polar Surface Area (TPSA) are essential for predicting the Absorption, Distribution, Metabolism and Excretion (ADME) properties of investigational molecules.[24] Compliance of a molecule with these physicochemical parameters is critical for determining its success.[37] SwissADME uses OpenBabel v.2.3.0 and a fragment-based approach to estimate the Polar Surface Area (PSA) for calculating ADME features. The HDAC2 inhibitor Entinostat, with a Molecular Weight of 376.4 g/mol and FCsp3 of 0.28, served as a reference. These insights into physicochemical properties significantly contribute to the rapid evaluation and prediction of ADME profiles for potential ligands (Table 2).[23,24]

Lipophilicity Assessment of Ligands and Reference Molecule Entinostat

The evaluation of a drug's lipophilicity is of paramount importance in revealing its capacity to dissolve in lipids or fats, offering valuable information on potential interactions and the drug's absorption within lipid-rich environments, which in turn influences its pharmacokinetic behavior within the body. Lipophilicity is typically measured using the Partition coefficient (P), which represents the ratio of the drug concentration in a nonpolar solvent (octanol) to that in a polar solvent (water).[38] A higher partition coefficient or lipophilicity indicates a higher likelihood of drug distribution and retention in lipid-rich tissues. Achieving optimal lipophilicity is essential for drug efficacy, necessitating a balanced approach to attain suitable pharmacokinetic properties for absorption, distribution, metabolism and excretion in the body.[39] Various computational and experimental methods have been employed in drug development to assess and optimize lipophilicity. The compounds examined exhibited a wide range of lipophilic characteristics, with iLOGP values ranging from 1.84 to 4, XLOGP values ranging from 2.02 to 4.04, WLOGP values ranging from 0.5 to 3.98 and MLOGP values ranging from 0.51 to 2.85. These values provide valuable insights into the lipophilic attributes of ligands and their potential impact on pharmacokinetics.

Solubility Characteristics of Ligands and Reference Molecule Entinostat

The evaluation of drug solubility is crucial for understanding its efficacy within the context of a biological system. Drugs with poor solubility present obstacles for formulation and delivery. Solubility refers to the maximum amount of substance that can dissolve in a solvent under particular conditions, including temperature and pressure.[40,41] SwissADME uses three methods

for solubility studies: ESOL, Ali and SILICOS-IT filters.[42,43] Upon assessment of solubility, the known inhibitor was identified to be poorly to moderately soluble, falling within the optimal range. Conversely, certain ligands exhibit moderate-to-good solubility. This information is essential for determining potential challenges in drug formulation and delivery and for identifying ligands with favorable solubility profiles for subsequent pharmaceutical development.

Pharmacokinetic Evaluation: Assessing Safety and Effectiveness

Pharmacokinetic evaluation is of paramount importance in determining the safety and effectiveness of potential drug candidates. This complex process involves examining the interactions of the compound with Permeability glycoprotein (P-gp) and Cytochrome P450 (CYP) enzymes as well as determining whether the compound is a substrate or non-substrate. The skin permeability coefficient (Kp) was quantified by using a regression model adapted from Potts and Guy.[44] A more negative Kp value indicates reduced skin permeability and decreased permeation through the skin barrier. Therefore, the negativity of Kp serves as an indicator of the restricted skin permeability of a compound. This parameter is a key metric for evaluating the viability of a drug candidate, specifically its ability to traverse the skin barrier.[45] The computed pharmacokinetic attributes of both the ligand and control molecules are outlined in Table 3.

In the realm of drug discovery and development, several guidelines or filters are employed to evaluate the drug-likeness of chemical compounds, including Lipinski's Rule of Five, Ghose's Rule, Veber's Rule, Egan's Rule and Muegge's rule.[46] These rules are invaluable tools for predicting the potential of a compound as an orally active drug. Although there are slight variations in the specific physicochemical properties considered among the rules, such as molecular weight, LogP value and number of hydrogen bond donors and acceptors, they collectively contribute to a comprehensive evaluation of a compound's suitability.[47]

Table 2: Physicochemical Properties Comparison of Ligands and the Established Inhibitor Entinostat.

Sl. No.	Molecules	MW	FCsp3	RB	HBA	HBD	MR	TPSA
1	Entinostat (Control)	376.41	0.04	6	6	2	129.47	140.98
2	MCULE-1047982559-0-12	490.53	0.28	7	6	2	141.64	118.34
3	MCULE-1153881170-0-3	478.86	0.38	7	8	2	119.54	130.84
4	MCULE-1537658116-0-1	499.47	0.29	10	8	3	124.45	131.42
5	MCULE-2009158975-0-4	495.98	0.48	5	8	2	133.86	135.55
6	MCULE-3797459988-0-5	497.93	0.25	6	5	2	143.44	111.29
7	MCULE-4334038893-0-3	455.44	0.27	10	8	2	114.47	118.82
8	MCULE-5097730104-0-3	475.84	0.04	6	6	2	129.47	140.98
9	MCULE-6503598615-0-2	477.44	0.21	8	9	2	121.01	128.46
10	MCULE-6610635460-0-144	493.95	0.25	7	6	2	136.76	124.33
11	MCULE-6885931637-0-1	496.96	0.33	10	7	3	126.29	134.45

Table 3: Comparative Pharmacokinetic Parameters of Ligands and Reference Inhibitor Entinostat.

Sl. No.	Ligands	CYP1A2	CYP2C19	CYP2C9	CYP2D6	CYP3A4
		Inhibitor				
1	Entinostat (Control)	Yes	Yes	Yes	Yes	Yes
2	MCULE-1047982559-0-12	No	Yes	Yes	Yes	Yes
3	MCULE-1153881170-0-3	No	No	No	No	Yes
4	MCULE-1537658116-0-1	No	No	Yes	No	Yes
5	MCULE-2009158975-0-4	No	Yes	Yes	No	Yes
6	MCULE-3797459988-0-5	No	No	Yes	No	Yes
7	MCULE-4334038893-0-3	No	Yes	Yes	Yes	Yes
8	MCULE-5097730104-0-3	No	Yes	Yes	No	Yes
9	MCULE-6503598615-0-2	No	No	Yes	Yes	Yes
10	MCULE-6610635460-0-144	No	Yes	Yes	Yes	Yes
11	MCULE-6885931637-0-1	No	Yes	Yes	Yes	Yes

Table 4: Drug Likeness Comparison of Ligands and Established Inhibitor Entinostat.

Sl. No.	Ligand	Lipinski	Ghose	Veber	Egan	Muegge
		Violations				
1	Entinostat (Control)	0	0	0	0	0
2	MCULE-1047982559-0-12	0	2	0	0	0
3	MCULE-1153881170-0-3	0	0	0	0	0
4	MCULE-1537658116-0-1	0	1	0	0	0
5	MCULE-2009158975-0-4	0	2	0	1	0
6	MCULE-3797459988-0-5	0	2	0	0	0
7	MCULE-4334038893-0-3	0	0	0	0	0
8	MCULE-5097730104-0-3	0	0	1	1	0
9	MCULE-6503598615-0-2	0	0	0	0	0
10	MCULE-6610635460-0-144	0	2	0	0	0
11	MCULE-6885931637-0-1	0	1	0	1	0

Lipinski's Rule of Five (RO5) assesses a compound based on four key properties: molecular weight, lipophilicity, hydrogen bond donors and hydrogen bond acceptors. Veber's rule centers on the oral bioavailability of a compound, specifically taking into account the number of rotatable bonds. Egan's rule evaluates oral availability based on molecular weight, LogP and hydrogen bond acceptors. Muegge's rule encompasses a range of properties, including molecular weight, lipophilicity and number of hydrogen bond donors and acceptors (Table 4). Collectively, these rules facilitate the assessment of drug-likeness of compounds, providing valuable insights into the drug development process.

Analysis of Medicinal Chemistry Attributes for Ligands and Known Inhibitor Entinostat

In the domain of drug discovery, the term Pan-Assay Interference Compounds (PAINS) refers to chemical substances that have the ability to disrupt a variety of biological assays, potentially resulting in false-positive outcomes in high-throughput screening. These substances, known as hits, exhibit nonspecific activity, leading to unwanted interactions with assay components. Notably, PAINS compounds lack specificity for a particular target and display activity in a wide range of biological assays.[48] To address this challenge, structural filters called Brenk alerts or filters have been developed. These filters were specifically designed to identify problematic compounds in virtual or high-throughput screening campaigns during drug discovery. Like other medicinal chemistry filters such as PAINS, Brenk alerts target-specific structural motifs identified through the analysis of compounds exhibiting undesirable assay interference properties. In the context of drug discovery, lead compounds, which are early-stage drug candidates with promising biological activity, undergo scrutiny for lead-likeness. This evaluation is dependent on criteria that encompass molecular weight, lipophilicity, hydrogen bond donors and acceptors, number of rotatable bonds and topological polar surface area.[38] It is essential to emphasize that these lead-likeness criteria function as guidelines rather than strict rules and are subject to variability based on the specific context and target class (Table 5). These attributes collectively contribute to the meticulous assessment of compounds during the drug discovery and development phases.

Molecular Dynamics Simulation Analysis: Evaluating Docked Complex Stability

To assess the stability of the docked complexes, Molecular Dynamics Simulation (MDS) was utilized, resulting in the generation of a graphical representation that displays the Root Mean Square Deviation (RMSD), Root Mean Square Fluctuation (RMSF) and Radius of Gyration. This analysis method is crucial for obtaining valuable insights into the dynamic behavior and stability of docked complexes throughout the simulation period.[28]

RMSD, RMSF and Rg Analysis of Docked Complexes

The Root Mean Square Deviation (RMSD) is a metric commonly used to quantify the square of the quadratic mean of the differences between the expected and actual values within a sample. It has been extensively employed to evaluate the stability of docked complexes. In this study, the RMSD values for the Cα atoms of HDAC2-MCULE-5097730104-0-3, HDAC2-MCULE-1047982559-0-12 and HDAC2-Entinostat complexes were determined over duration of approximately 5 ns. Specifically, the RMSD values for the HDAC2-MCULE-5097730104-0-3 and HDAC2-MCULE-1047982559-0-12 complexes were measured at 0.26 nm and 0.34 nm, respectively, while the RMSD value for the reference molecule HDAC2-Entinostat was recorded at 0.28 nm (Figure 4A).

The Root Mean Square Fluctuation (RMSF) is a valuable analytical tool for evaluating the dynamic flexibility of docked complexes. It is commonly employed to quantify variations by comparing initial and final fluctuations. The average RMSF values for the

Table 5: Comparative Analysis of Medicinal Chemistry Attributes in Ligands and Reference Inhibitor Entinostat.

Sl. No.	Molecules	PAINS alerts	Brenk alerts	Lead likeness violations	Synthetic Accessibility
1	Entinostat (Control)	0	1	2	2.67
2	MCULE-1047982559-0-12	0	0	1	4.16
3	MCULE-1153881170-0-3	0	1	1	4.4
4	MCULE-1537658116-0-1	0	0	2	3.6
5	MCULE-2009158975-0-4	0	0	1	3.52
6	MCULE-3797459988-0-5	0	2	1	4.13
7	MCULE-4334038893-0-3	0	0	2	3.58
8	MCULE-5097730104-0-3	0	2	1	2.78
9	MCULE-6503598615-0-2	0	0	2	4.68
10	MCULE-6610635460-0-144	0	0	2	4.03
11	MCULE-6885931637-0-1	0	0	2	3.59

docked complexes, HDAC2-MCULE-5097730104-0-3 (0.52 nm), HDAC2-MCULE-1047982559-0-12 (1.31 nm) and the control HDAC2-Entinostat (0.65 nm), provide essential information about the structural fluctuations observed during molecular dynamics simulations, as depicted in Figure 4B.

The fact that the observed decrease in the Radii of gyration (Rg) for the docked complexes is indicative of increased compactness is a noteworthy observation. The average Rg values for HDAC2-MCULE-5097730104-0-3, HDAC2-MCULE-1047982559-0-12 and the control HDAC2-Entinostat are 3.02 nm, 3.00 nm and 3.02 nm, respectively (as depicted in Figure 4C). This analysis provides essential insights into the structural attributes and compactness of the docked complexes during molecular dynamics simulations, offering valuable information for future investigations.

This study systematically employed Pfizer's Lipinski's Rule of Five criteria in a comprehensive screening process to identify potential drug candidates targeting cancer progression with a specific focus on HDAC2. From an initial pool of over two million candidates, 100 promising ligands were identified. Subsequent evaluations, which considered the binding free energy and hydrogen bond formation, reduced the selection of ten outstanding molecules. These findings played a crucial role in the refinement process, ultimately leading to the identification of two lead ligands that exhibited binding affinities comparable to those of the control drug entinostat. Docking simulations and toxicity assessments provided valuable insights into the interactions between these ligands and HDAC2 binding pocket. Structural interactions, as depicted in Figures 4 and 6, outlined the bonding modes and residues involved by MCULE-5097730104-0-3 and MCULE 1047982559-0-12. These findings provide the foundation for associating these interactions with potential drug candidates. MCULE-5097730104-0-3 demonstrated an inability to penetrate either the HIA or BBB barrier, indicating lower stability. In contrast, MCULE 1047982559-0-12 successfully penetrated the HIA barrier but failed to penetrate the BBB. With regard to medicinal chemistry attributes, MCULE-5097730104-0-3 showed two Brenk alerts and one lead-likeness violation, while MCULE 1047982559-0-12 had only one lead-likeness violation. Both ligands exhibited greater synthetic accessibility than entinostat (control). In terms of stability assessment through Molecular Dynamics (MD) simulations, MCULE-5097730104-0-3 demonstrated exceptional stability in the docking complex with HDAC2.

In brief, both MCULE-5097730104-0-3 and MCULE 1047982559-0-12 demonstrated promising characteristics as potential therapeutic agents for cancer treatment. Their robust binding affinities, favorable properties for oral administration and stability upon interaction with the target protein make them appealing candidates. In contrast, MCULE-5097730104-0-3 exhibited higher stability in molecular dynamics simulations and a lower number of violations in medicinal chemistry attributes, indicating that it may be a more favorable candidate than MCULE 1047982559-0-12 and even the reference compound, entinostat. Further optimization and development are necessary to fully harness the potential of these lead compounds in the pursuit of effective cancer treatment.

DISCUSSION

The Structure-Based Virtual Screening (SBVS) results in this study, employing a comprehensive screening protocol through the Mcule online drug discovery platform, have yielded promising candidates for targeting cancer progression, explicitly focusing on HDAC2. The screening process involved the initial acquisition of a vast dataset of 2,208,042 ligand molecules, which was subsequently refined based on stringent criteria, including adherence to Lipinski's Rule of Five (RO5), drug-likeness parameters and considerations of N and O atoms. This meticulous selection process led to the identification of two investigational ligands, MCULE-5097730104-0-3 and

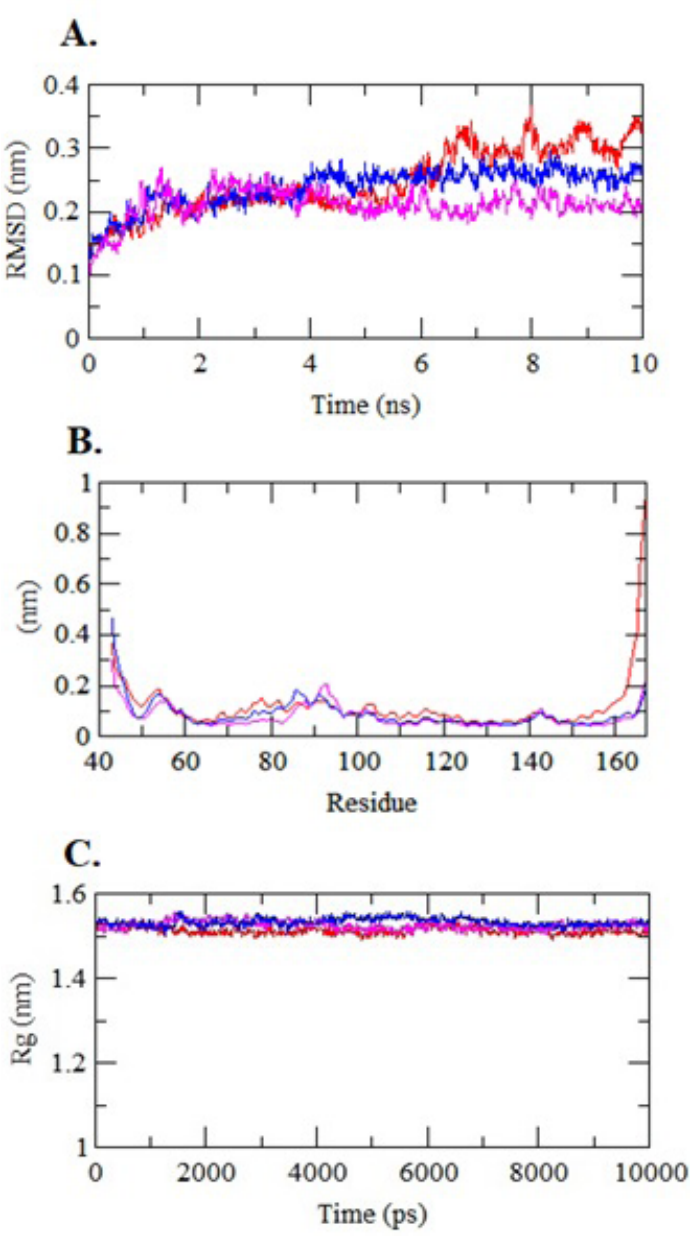

Figure 4: (A) The figure illustrates the Root Mean Square Deviation (RMSD) plot for three different complexes: HDAC2-MCULE-5097730104-0-3 (magenta), HDAC2-MCULE-1047982559-0-12 (red) and HDAC2-Entinostat (control) (blue). The plot visually represents the structural stability of each complex over the course of the molecular dynamics simulation. The distinct colors correspond to different ligands, allowing for a comparative analysis of their dynamic behavior and stability. (B) The graph depicts the Root Mean Square Fluctuation (RMSF) plot for three different complexes: HDAC2-MCULE-5097730104-0-3 (magenta), HDAC2-MCULE-1047982559-0-12 (red) and HDAC2-Entinostat (control) (blue). The plot visually represents the flexibility and variations in structural fluctuations of each complex throughout the Molecular Dynamics Simulation. Each colour corresponds to a different ligand, facilitating a comparative analysis of their dynamic behaviour. (C) The figure illustrates the Radius of Gyration (Rg) plot for three different complexes: HDAC2-MCULE-5097730104-0-3 (magenta), HDAC2-MCULE-1047982559-0-12 (red) and HDAC2-Entinostat (control) (blue). The plot visually represents the compactness and structural characteristics of each complex throughout the Molecular Dynamics Simulation. Each colour corresponds to a different ligand, enabling a comparative analysis of their overall structural behaviour.

MCULE-1047982559-0-12, characterized by ΔG values of -9.7 kcal/mol and -9.2 kcal/mol, respectively, which surpassed the binding free energy of the control molecule entinostat (-8.5 kcal/mol).

Toxicity profiling and assessment of the binding free energy were crucial steps in refining the selection of ligands. Out of the initial 100 ligands, only ten demonstrated the absence of toxic moieties or problematic scaffolds, providing a pool of ligands for further consideration. Molecular docking analysis using DockThor revealed that both lead ligands exhibited favorable binding affinities and hydrogen bond interactions with HDAC2 residues compared to the reference molecule entinostat. MCULE-5097730104-0-3 and MCULE-1047982559-0-12 demonstrated three and one hydrogen bonds, respectively, in contrast to the entinostat, which displayed three hydrogen bonds.

Evaluating Human Intestinal Absorption (HIA) and Blood-Brain Barrier (BBB) permeation using the Egan-Egg filtration model indicated plausible HIA permeation for all ligands, but none demonstrated BBB permeability. This information is crucial for rational drug design, indicating potential limitations in the ligands' ability to access the central nervous system. Physicochemical characteristics were analyzed to predict ADME properties, including molecular weight, FCsp3 hybridization, rotatable bonds, hydrogen bond acceptor/donor and total polar surface area. Lipophilicity assessment revealed a wide range of values for the ligands, providing insights into their potential interactions and absorption within lipid-rich environments.

The solubility characteristics of the ligands were assessed using multiple methods, highlighting variations in solubility profiles among the ligands and the reference molecule entinostat. Pharmacokinetic evaluation, including interactions with Permeability glycoprotein (P-gp) and Cytochrome P450 (CYP) enzymes, as well as skin permeability coefficient (Kp), was performed, contributing to the understanding of the safety and effectiveness of the potential drug candidates.

The adherence to drug-likeness rules, such as Lipinski's Rule of Five, Veber's Rule and others, was emphasized throughout the study. Medicinal chemistry attributes, including the identification of Pan-Assay Interference Compounds (PAINS) and the application of lead-likeness criteria, provided additional layers of scrutiny for the selected ligands. Molecular Dynamics Simulation (MDS) analysis further assessed the stability of the docked complexes, revealing RMSD, RMSF and Rg values. The findings from MDS indicated the stability and structural fluctuations of the ligand-HDAC2 complexes over a simulated period.

In summary, this study's systematic application of a multi-faceted approach has identified two lead ligands, MCULE-5097730104-0-3 and MCULE-1047982559-0-12, as promising candidates for further consideration in cancer drug development. Their robust binding affinities, favorable pharmacokinetic properties and

stability in molecular dynamics simulations position them as potential therapeutic agents. However, further optimization and development are necessary to fully exploit their potential in pursuing effective cancer treatment. The detailed analysis presented in this study provides a comprehensive foundation for advancing these lead compounds in the drug development pipeline.

CONCLUSION

The substantial global burden of cancer has prompted researchers to concentrate on elucidating its etiology and pathophysiology. The urgency to develop therapeutic agents to eradicate and impede cancer progression aligns with the current global demands. Cancer is characterized by cellular behavior irregularities resulting from intricate interactions within the cellular environment. Its etiology involves a multifaceted interplay of various factors. Clinical trials for cancer treatment face significant obstacles, such as the limited efficacy of lead compounds, issues in trial design, cancer heterogeneity, resistance, relapse, shifts in the competitive landscape, difficulties in patient retention, safety concerns associated with investigational treatments and complexities in trial design. A thorough evaluation of several ligands identified MCULE-5097730104-0-3 as the most promising drug candidate.

This determination is derived from a meticulous assessment of parameters, such as binding affinity, pharmacokinetics and potential therapeutic effects. MCULE-5097730104-0-3 exhibits superior characteristics in these domains compared to other ligands, indicating its potential as an exceptionally effective drug candidate. This conclusion was corroborated by a comprehensive analysis of the data, which highlighted the outstanding performance of MCULE-5097730104-0-3 among the scrutinized candidates.

ACKNOWLEDGEMENT

The authors recognize with much obliged for Deanship Research at the Department of Clinical Biochemistry, College of Medicine, King Khalid University, Abha, Saudi Arabia.

CONFLICT OF INTEREST

The authors declare that they have nothing to disclose.

ABBREVIATIONS

HDAC2: Histone deacetylase 2; **ADME:** Absorption, Distribution, Metabolism and Excretion; **SBVS:** Structure-Based Virtual Screening; **MD:** Molecular docking; **RMSD:** Root Mean Square Deviation; **RMSF:** Root Mean Square Fluctuation; **Rg:** Radius of Gyration; **HAT:** Histone acetyltransferase.

SUMMARY

Cancer's global burden necessitates research on its etiology and pathophysiology. Clinical trials face challenges like limited efficacy, design issues, cancer heterogeneity, resistance, relapse and safety concerns. MCULE-5097730104-0-3 is identified as the most promising drug candidate, addressing these obstacles. MCULE-5097730104-0-3, a very effective drug candidate, outperformed other ligands in terms of binding affinity, pharmacokinetics and therapeutic effects, as evidenced by detailed data analysis.

REFERENCES

1. World Health Organization. Latest global cancer data: cancer burden rises to 19.3 million new cases and 10.0 million cancer deaths in 2020 (December). International Agency for Research on Cancer; 2020.
2. Sung H, Ferlay J, Siegel RL, Laversanne M, Soerjomataram I, Jemal A, *et al.* Global cancer statistics 2020: GLOBOCAN estimates of incidence and mortality worldwide for 36 cancers in 185 countries. CA Cancer J Clin. 2021;71(3):209-49. doi: 10.3322/caac.21660, PMID 33538338.
3. Siegel RL, Miller KD, Wagle NS, Jemal A. Cancer statistics, 2023. CA A Cancer J Clinicians. 2023;73(1):17-48. doi: 10.3322/caac.21763.
4. World Health Organization. Cancer WHO. Cancer. 2021.
5. Ferlay J, Ervik M, Lam F, Colombet M, Mery L, Piñeros M, *et al.* Global cancer observatory. Cancer Today. 2020;6:68.
6. Nenclares P, Harrington KJ. The biology of cancer. Medicine. 2020;48(2):67-72. doi: 10.1016/j.mpmed.2019.11.001.
7. Wolin KY, Colditz GA. Cancer and beyond: healthy lifestyle choices for cancer survivors. J Natl Cancer Inst. 2013;105(9):593-4. doi: 10.1093/jnci/djt052, PMID 23492347.
8. Josfeld L, Krüger L, Büntzel J, Zomorodbakhsch B, Hübner J. Self-efficacy in relation to the use of complementary and alternative medicine, lifestyle choices and cancer aetiology. J Cancer Res Clin Oncol. 2022;148(10):2707-15. doi: 10.1007/s00432-021-03857-3, PMID 34812932.
9. Zhou JJ, Feng XL, Zhou Z. Chromatin assembly of histone variants. Prog Biochem Biophys. 2015;42.
10. Bondarev AD, Attwood MM, Jonsson J, Chubarev VN, Tarasov VV, Schiöth HB. Recent developments of HDAC inhibitors: emerging indications and novel molecules. Br J Clin Pharmacol. 2021;87(12):4577-97. doi: 10.1111/bcp.14889, PMID 33971031.
11. Borcoman E, Kamal M, Marret G, Dupain C. Castel-ajgal Z, Le Tourneau C. Cancers. 2019. HDAC inhibition to prime immune checkpoint inhibitors;14: 2022.
12. Bank PD. RCSB PDB: homepage. Rcsb Pdb.
13. Burley SK, Bhikadiya C, Bi C, Bittrich S, Chao H, Chen L, *et al.* RCSB Protein Data bank: tools for visualizing and understanding biological macromolecules in 3D. Protein Sci. 2022;31(12):e4482. doi: 10.1002/pro.4482, PMID 36281733.
14. Brooks BR, Brooks CL, Mackerell AD, Nilsson L, Petrella RJ, Roux B, *et al.* (2009). CHARMM: The biomolecular simulation program. J Comput Chem. 30(10).
15. Karami TK, Hailu S, Feng S, Graham R, Gukasyan HJ. Eyes on Lipinski's rule of five: A new "rule of thumb" for physicochemical design space of ophthalmic drugs. J Ocul Pharmacol Ther. 2022;38(1):43-55. doi: 10.1089/jop.2021.0069, PMID 34905402.
16. Lipinski CA, Lombardo F, Dominy BW, Feeney PJ. Experimental and computational approaches to estimate solubility and permeability in drug discovery and development settings. Adv Drug Deliv Rev. 2012;64.
17. Kim S, Chen J, Cheng T, Gindulyte A, He J, He S, *et al.* PubChem 2023 update. Nucleic Acids Res. 2023;51(D1):D1373-80. doi: 10.1093/nar/gkac956, PMID 36305812.
18. Kim S, Chen J, Cheng T, Gindulyte A, He J, He S, *et al.* PubChem in 2021: new data content and improved web interfaces. Nucleic Acids Res. 2021;49(D1):D1388-95. doi: 10.1093/nar/gkaa971, PMID 33151290.
19. Butt SS, Badshah Y, Shabbir M, Rafiq M. Molecular docking using chimera and autodock vina software for nonbioinformaticians. JMIR bioinform biotech. 2020;1(1).
20. Rizvi SMD, Shakil S, Haneef M. A simple click by click protocol to perform docking: autodock 4.2 made easy for non-bioinformaticians. Excli J. 2013;12:831-57. PMID 26648810.
21. Eberhardt J, Santos-Martins D, Tillack AF, Forli S. AutoDock vina 1.2.0: new docking methods, expanded force field and python bindings. J Chem Inf Model. 2021;61(8):3891-8. doi: 10.1021/acs.jcim.1c00203, PMID 34278794.
22. Morris GM, Goodsell DS, Huey R, Olson AJ. Distributed automated docking of flexible ligands to proteins: parallel applications of AutoDock 2.4. J Comput Aid Mol Des. 1996;10(4):293-304. doi: 10.1007/BF00124499, PMID 8877701.
23. Shen J, Cheng F, Xu Y, Li W, Tang Y. Estimation of ADME properties with substructure pattern recognition. J Chem Inf Model. 2010;50(6):1034-41. doi: 10.1021/ci100104j, PMID 20578727.

24. Deb S, Reeves AA, Hopefl R, Bejusca R. ADME and pharmacokinetic properties of remdesivir: its drug interaction potential. Pharmaceuticals (Basel). 2021;14(7). doi: 10.3390/ph14070655, PMID 34358081.
25. Shou WZ. Current status and future directions of high-throughput ADME screening in drug discovery. J Pharm Anal. 2020;10(3):201-8. doi: 10.1016/j.jpha.2020.05.004, PMID 32612866.
26. Sharma S, Kumar P, Chandra R. Applications of BIOVIA materials studio, LAMMPS and GROMACS in various fields of science and engineering. In: Molecular Dynamics simulation of nanocomposites using BIOVIA materials studio, Lammps and Gromacs; 2019.
27. Irrgang ME, Davis C, Kasson PM. gmxapi: a GROMACS-native Python interface for molecular dynamics with ensemble and plugin support. PLOS Comput Biol. 2022;18(2):e1009835. doi: 10.1371/journal.pcbi.1009835, PMID 35157693.
28. Tandon R, Chandra S, Baharia RK, Misra P, Das S, Rawat K, *et al.* Molecular, biochemical characterization and assessment of immunogenic potential of cofactor-independent phosphoglycerate mutase against *Leishmania donovani*: A step towards exploring novel vaccine candidate. Parasitology. 2018;145(4):508-26. doi: 10.1017/S0031182017001160, PMID 28691653.
29. Maia EHB, Assis LC, de Oliveira TA, da Silva AM, Taranto AG. Structure-based virtual screening: from classical to artificial intelligence. Front Chem. 2020;8:343. doi: 10.3389/fchem.2020.00343, PMID 32411671.
30. Cheng T, Li Q, Zhou Z, Wang Y, Bryant SH. Structure-based virtual screening for drug discovery: A problem-centric review. AAPS J. 2012;14(1):133-41. doi: 10.1208/s12248-012-9322-0, PMID 22281989.
31. Vo AH, Van Vleet TR, Gupta RR, Liguori MJ, Rao MS. An overview of machine learning and big data for drug toxicity evaluation. Chem Res Toxicol. 2020;33(1):20-37. doi: 10.1021/acs.chemrestox.9b00227, PMID 31625725.
32. Santos KB, Guedes IA, Karl ALM, Dardenne LE. Highly flexible ligand docking: benchmarking of the DockThor program on the leads-PEP protein-peptide data set. J Chem Inf Model. 2020;60(2):667-83. doi: 10.1021/acs.jcim.9b00905, PMID 31922754.
33. Kim Y, Park K, Kim YJ, Shin SW, Kim YJ, Choi C, *et al.* Immunomodulation of HDAC inhibitor entinostat potentiates the anticancer effects of radiation and PD-1 blockade in the murine lewis lung carcinoma model. Int J Mol Sci. 2022;23(24). doi: 10.3390/ijms232415539, PMID 36555180.
34. Lin J, Elkon J, Ricart B, Palmer E, Zevallos-Delgado C, Noonepalle S, *et al.* Phase I study of entinostat in combination with enzalutamide for treatment of patients with metastatic castration-resistant prostate cancer. Oncologist. 2021;26(12):e2136-42. doi: 10.1002/onco.13957, PMID 34427023.
35. Truong AS, Zhou M, Krishnan B, Utsumi T, Manocha U, Stewart KG, *et al.* Entinostat induces antitumor immune responses through immune editing of tumor neoantigens. J Clin Invest. 2021;131(16). doi: 10.1172/JCI138560, PMID 34396985.
36. Bucknall V, Mehdi A. The boiled-egg technique: a new method for obtaining femoral head autograft used in acetabular defect reconstruction. J Arthroplasty. 2013;28(8):1391-3. doi: 10.1016/j.arth.2012.10.026, PMID 23540538.
37. Daina A, Zoete V. A BOILED-egg to predict gastrointestinal absorption and brain penetration of small molecules. ChemMedChem. 2016;11(11):1117-21. doi: 10.1002/cmdc.201600182, PMID 27218427.
38. Waring MJ. Lipophilicity in drug discovery. Expert Opin Drug Discov. 2010;5(3):235-48. doi: 10.1517/17460441003605098, PMID 22823020.
39. Arnott JA, Planey SL. The influence of lipophilicity in drug discovery and design. Expert Opin Drug Discov. 2012;7(10):863-75. doi: 10.1517/17460441.2012.714363, PMID 22992175.
40. Savjani KT, Gajjar AK, Savjani JK. Drug solubility: importance and enhancement techniques. ISRN Pharm. 2012; 2012:195727. doi: 10.5402/2012/195727, PMID 22830056.
41. Ali J, Camilleri P, Brown MB, Hutt AJ, Kirton SB. Revisiting the general solubility equation: *in silico* prediction of aqueous solubility incorporating the effect of topographical polar surface area. J Chem Inf Model. 2012;52(2):420-8. doi: 10.1021/ci200387c, PMID 22196228.
42. Delaney JS. ESOL: estimating aqueous solubility directly from molecular structure. J Chem Inf Comput Sci. 2004;44(3):1000-5. doi: 10.1021/ci034243x, PMID 15154768.
43. Daina A, Michielin O, Zoete V. SwissADME: A free web tool to evaluate pharmacokinetics, drug-likeness and medicinal chemistry friendliness of small molecules. Sci Rep. 2017;7:42717. doi: 10.1038/srep42717, PMID 28256516.
44. O'Hara K. Paediatric pharmacokinetics and drug doses. Aust Prescr. 2016;39(6):208-10. doi: 10.18773/austprescr.2016.071.
45. Choi YA, Song IS, Choi MK. Pharmacokinetic drug-drug interaction and responsible mechanism between memantine and cimetidine. Pharmaceutics. 2018;10(3). doi: 10.3390/pharmaceutics10030119, PMID 30082658.
46. Veber DF, Johnson SR, Cheng HY, Smith BR, Ward KW, Kopple KD. Molecular properties that influence the oral bioavailability of drug candidates. J Med Chem. 2002;45(12):2615-23. doi: 10.1021/jm020017n.
47. Muegge I, Heald SL, Brittelli D. Simple selection criteria for drug-like chemical matter. J Med Chem. 2001;44(12):1841-6. doi: 10.1021/jm015507e.
48. Nehal M, Khan I, Khatoon J, Akhtar S, Ahmad Khan MK. Metabolomics of medicinal and aromatic plants. Ethnobotany and ethnopharmacology of medicinal and aromatic plants: steps towards drug discovery; 2023.

Cite this article: Patel AA, Alothaid H, Mallick AK, Mirdad RT, Mirdad MT, Mirdad MT, *et al*. Inhibiting Cancer Progression through Targeting HDAC2 with Novel Ligands: A Dynamic Insights through Virtual Screening and Simulation. Indian J of Pharmaceutical Education and Research. 2024;58(3):802-13.